The Effect of Talus Osteochondral Defects of Different Area Size on Ankle Joint Stability: A Finite Element Analysis

Jia Li
Chinese PLA General Hospital
Yezhou Wang
Tongji University
Yu Wei
Chinese PLA General Hospital
Dan Kong
Chinese PLA General Hospital
Yuan Lin
the Second Affiliated Hospital of Harbin Medical University
Duanyang Wang
the Second Affiliated Hospital of Harbin Medical University
Shi Cheng
the Second Affiliated Hospital of Harbin Medical University
Pengbin Yin
Chinese PLA General Hospital
Min Wei (weimin301@126.com)
Chinese PLA General Hospital

Research Article

Keywords: Ankle Injuries, Osteochondral lesion of the talus (OLT), Finite Element Analysis（FEA), Ankle Joint Instability

Posted Date: July 15th, 2021

DOI: https://doi.org/10.21203/rs.3.rs-677981/v1

Abstract

(1) Background: Osteochondral lesion of the talus (OLT) is one of the common ankle injuries, which will lead to biomechanical changes in the ankle joint and ultimately affect the ankle function. The finite element analysis (FEA) was used to clarify the effect of talus osteochondral defects in different depths on the stability of the ankle joint. However, there is no clear research about the area of talus osteochondral defects that should be intervened in time. In this research, FEA is used to simulate the effect of different areas size of talus osteochondral defect on the stress and stability of ankle joint under a certain depth defect.;

(2) Methods: The different area size (Normal, 2 mm* 2 mm, 4 mm* 4 mm, 6 mm* 6 mm, 8 mm* 8 mm, 10 mm* 10 mm, 12 mm* 12 mm) of osteochondral defects three-dimensional finite element model was established to simulate and calculate joint stress and displacement of the articular surface of the distal tibia and the proximal talus while the ankle joint was in the push-off phase, midstance phase and heel-strike phase;

(3) Results: When OLT occurred, the contact pressure of articular surface, the equivalent stress of the proximal talus, tibial cartilage and talus cartilage did not change significantly with the increase of osteochondral defect area size in heel-strike phase below 6 mm * 6 mm, it increased gradually from 6 mm * 6 mm in midstance phase and push-off phase, and reached the maximum when the defect area size is 12 mm * 12 mm. The talus displacement also has the same tendency.;

(4) Conclusions: The effect of cartilage area size defects of the talus on the biomechanics of the ankle is obvious especially in the midstance phase and push-off phase. When the defect size reaches 6 mm * 6 mm, the most obvious change in the stability of the ankle joint occurs, and the effect does not increase linearly with the increase in the depth of the defect.

1. Introduction

Ankle joint injuries represent a major health care problem. Ankle joint injuries account for 20% of joint injuries and have a high recurrence rate [1]. More importantly, acute or recurrent ankle trauma is closely related to the occurrence of post-traumatic ankle osteoarthritis [2]. Osteochondral lesion of the talus (OLT) is one of the common ankle injuries[3–4], for the treatment of OLT, conservative treatment is mainly suitable for patients with mild clinical symptoms, small injury area, stable avulsion bone without fracture displacement, and chronic talus osteochondral injury, such as Hepple type I ~ II[5]. Hepple type II ~ V type symptoms are obvious, conservative treatment is ineffective for more than 3 to 6 months, or the damage area is large, and the acute separation and displacement of the OLT requires surgical treatment[6–8]. It can be seen from the above that, whether it is conservative treatment or surgical treatment, there is no clear quantitative indicator for the size of the area. Therefore, how to choose the treatment method for OLT with different defect areas is a difficult problem for orthopedic surgeons.

For OLT, there are usually includes depth defects and area defects. Regarding the impact of depth defects, our research team used finite element analysis (FEA) found that when the depth of the defect exceeds 3mm, the stability of the ankle joint is significantly affected [9]. At present, studies have pointed out that the area of talus osteochondral defect is an important factor affecting the stability of the ankle joint and the treatment effect [10], but about the size of the area defect, the literature suggests that the area defect diameter ≤ 10mm is poorly treated with microfracture surgery [11–12]. However, there is no relevant research that has clearly defined the impact of defects of less than 10mm diameter on the ankle joint stress and stability of the ankle joint. Therefore, understanding the impact of talus osteochondral defects of different sizes on the biomechanics and stability of the ankle joint is of great significance for the treatment of talus osteochondral defects.

By constructing a finite element model of the ankle joint, our group selected a normal cartilage model to simulate a 1 mm defect depth of the talus osteochondral defect. The area defect size is 2 mm * 2 mm, 4 mm * 4 mm, 6 mm * 6 mm, 8 mm * 8 mm, 10 mm * 10 mm, 12 mm * 12mm three-dimensional finite element analysis were performed to explore the influence of different defect areas sizes on the biomechanics and stability of the ankle joint.

2. Materials And Methods

Processing of the CT files and three-dimensional solid reconstruction

An image of the right ankle joint of an adult man in a neutral position was obtained by CT tomography (64 slices, SIEMENS, US), and the image was input into the 3D reconstruction software Mimics in the Dicom format to obtain a clear skeleton outline. After mask processing, the image was read in Geomagic (Geomagic,US) in the STL format, reverse engineering reconstruction was completed, and the 3D graphics in the IGES file format were generated (Fig. 1).

Construction of the working condition model

After the foot skeleton and foot contour were built, all ligaments were connected with lines in the physiological position, and a complete foot model was generated. According to the anatomical data of the joint surface, cartilage boundaries were established, and cartilage joints were built with Geomagic with an offset thickness of 1 mm. According to the requirements of the analysis, only the fibula and tibia of the calcaneal talus, as well as the related cartilages and ligaments, were required to be retained; thus, a relatively complete three-dimensional finite element model of the ankle joint of the normal adults was built. On the basis of the normal model, the talus cartilage was divided into 9 regions by the nine-grid partition method. Studies have shown that area 4 is the most common area for talus cartilage injuries [13, 14]. In this study, defects in the cartilage and subchondral bone in region 4 of the talus were simulated. Because the existing literature does not study the area size of finite element and talus injury, when we conduct finite element analysis, the experimental measurement depth 1mm, and the area defect size is 2 mm * 2 mm, 4 mm * 4 mm, 6 mm * 6 mm, 8 mm *8 mm, 10 mm *10 mm, 12 mm * 12 mm (Fig. 2).

Meshing

The assembled solid model was imported into Ansys Workbench (Ansys, USA), a Boolean operation was carried out, material parameters were assigned, contact was defined, and then, the grid division process was completed. The solid unit comprised Solid 187 and Solid 95, the ligament was a Link180 unit, and its nonlinear characteristics were set under tension without pressure (Fig. 3).

Material parameters and Contact Settings

All kinds of tissue materials involved in this model were simplified into isotropic homogeneous elastic materials, and the material parameters are listed in Table 1 and Table 2.

Table 1
Properties of the bone and cartilage materials

Material	Modulus of Elasticity (MPa)	Poisson's ratio
Bone	7300	0.3
Cartilage	12	0.42

Table 2
Material properties of the ligaments

Ligament	Modulus of Elasticity (MPa)	Poisson's ratio	Sectional area (mm^2)
AtiF	260	0.4	18.4
PtiF	260	0.4	18.4
AtaFi	255.5	0.4	12.9
PtaFi	216.5	0.4	21.9
CaTi	512	0.4	9.7
AtiTa	184.5	0.4	13.5
PtiTa	99.5	0.4	22.6
TiCa	512	0.4	9.7
TiNa	320.7	0.4	7.1

AtiF = Anterior tibiofibular ligament,PtiF = Posterior tibiofibular ligament□AtaFi = Anterior talofibular ligament□PtaFi = Posterior talofibular ligament□CaTi = Calcaneofibular ligament□AtiTa = Anterior tibial ligament□PtiTa = Posterior tibial talus ligament□TiCa = Tibiocalcanean ligament□TiNa = Tibionavicular ligament

The settings of the contact between the components were set according to the actual condition. The cartilage was bound to the corresponding bones, and the friction coefficient between the articular surfaces of the cartilage was 0.01.

Applying loads and constraints

The grid direction of the corresponding sites of the calcaneus and scaphoid was constrained so that the degree of freedom was 0. Three gait patterns were selected for analysis according previous studies, as shown below, and it was assumed that the body weight was 600 N and the foot length was 25.4 cm (Fig. 4). After the model was established, it was verified that it was close to those in previous studies. [8–9].

Experimental groups and data acquisition process

After the above model was established, 7 groups were established for the experiment: the normal talus osteochondral group and groups the area defect size is 2 mm * 2 mm, 4 mm * 4 mm, 6 mm * 6 mm, 8 mm *8 mm, 10 mm *10 mm, 12 mm * 12 mm. In each group, the finite element method and the above model were used to simulate the stress on the ankle joint when it was in the push-off phase, midstance phase and heel-strike phase to determine the contact pressure on the joint surface, the equivalent stress of the cartilage of the proximal talus and distal tibia in each phase, and the displacement of the talus. The stress, contact state and displacement of each component of the ankle joint in the different groups were observed to determine its maximum value and location. The maximum pressure was recorded as the experimental data and analyzed to obtain the column diagram, and the changes in pressure were discussed.

3. Results

Using a 3D finite element simulation of osteochondral defects at different area sizes of the talus, the following was found:

3.1. Contact pressure of the articular surface and Displacement of the talus

When the defect size was below 6 mm * 6 mm, the contact pressure of the articular surface and displacement of the talus increased with increasing osteochondral defect area sizes in the heel-strike phase, but the stress and displacement did not change significantly. When the defect size was above 6 mm * 6mm,the stress and displacement increased with increasing area sizes of the defect in the midstance and push-off phases. Stress reached the highest level (8.7896 Mpa and 6.2716 MPa, respectively) in the midstance and push-off phase when the defect size was 12 mm * 12 mm. The highest displacement was also at the 6 mm * 6 mm in the midstance and push-off phase (8.3045mm and 7.3983mm, respectively) (Table 3).

Table 3
Pressure of the ankle joint surface and displacement of the talus in the heel-strike phase, midstance phase and push-off phases

Parameters	Contact pressure			Displacement of the talus		
	Heel-strike phase	Midstance phase	Push-off phase	Heel-strike phase	Midstance phase	Push-off phase
Normal	3.7599	4.8247	4.6199	1.9665	5.8657	5.3314
2×2×1	3.7737	4.8719	4.4613	1.9814	5.9118	5.3883
4×4×1	3.9324	5.0558	4.508	1.9866	6.0754	5.5299
6×6×1	3.6558	5.5525	5.3059	2.0156	6.291	5.8229
8×8×1	3.9323	6.3312	6.2716	2.2125	7.0086	6.3655
10×10×1	4.902	7.1888	7.3397	2.2968	7.6493	6.8185
12×12×1	4.6543	8.7896	9.6693	2.6559	8.3045	7.3983

3.2 *The equivalent stress of the proximal talus, tibial cartilage and talus cartilage*

These three indexes had the same trendcy as the contact pressure of the articular surface and displacement of the talus, it means that when the defect size is below 6 mm * 6 mm, the equivalent stress of the proximal talus, tibial cartilage and talus cartilage were increased with increasing osteochondral defect area sizes in the heel-strike phase, but the stress and displacement did not change significantly; when the defect size was above 6 mm * 6 mm, the equivalent stress increased with increasing area sizes of the defect in the midstance and push-off phases. Stress reached the highest level in the midstance and push-off phase when the defect size was 12 mm * 12 mm (Table 4).

Table 4
Equivalent stress of the upper talus, tibial cartilage and talus cartilage in the heel-strike phase, midstance phase and push-off phases

Parameters	Equivalent stress of the upper talus			Equivalent stress of tibial cartilage			Equivalent stress of talus cartilage		
	Heel-strike phase	Midstance phase	Push-off phase	Heel-strike phase	Midstance phase	Push-off phase	Heel-strike phase	Midstance phase	Push-off phase
Normal	2.106	4.4531	3.1456	1.6477	2.479	2.2873	2.2804	2.7872	2.4853
2×2×1	2.1009	4.4679	3.1722	2.311	5.0803	2.3641	1.8974	3.0599	2.9754
4×4×1	2.1125	4.617	3.246	2.3166	5.1477	2.4983	1.8261	3.5431	3.2516
6×6×1	2.129	5.1434	3.5119	1.6715	5.2665	2.9691	1.85	4.3454	4.1944
8×8×1	2.183	6.1385	4.3914	2.2682	5.5435	3.7991	2.4564	5.7413	5.2679
10×10×1	2.2712	7.5035	5.4651	3.1235	5.7034	4.0634	3.08	8.0266	6.8207
12×12×1	2.2621	8.3939	6.1956	2.6804	8.9997	8.1271	3.0477	8.5985	8.2563

4. Discussion

The most important findings of the study of the talus cartilage defect models with different areas in the IV area of the talus cartilage: 1. In the heel-strike phase, the stress of the talus cartilage defect in different areas did not change much; 2. In the midstance and push-off phase, when the defect area was below 6 mm * 6 mm, the changed of stress and displacement in each group were not obvious, but when the defect area size was above 6 mm*6 mm, the stress and changed of stress and displacement showed an obvious positive growth trend. When the defect area was 12mm*12 mm, the stress and displacement of each group reached maximum value.

The ankle joint surface of the talus plays an important role in the biomechanics of the ankle joint [15]. Previous studies have used biomechanics tests in cadaveric bone to simulate defects of 6 mm, 8 mm, 10 mm, and 12 mm to clarify the effect of defects on the stress of the ankle joint. The study only simulated neutral position and 15° plantar flexion position and it found that when it is larger than 10mm, the stress gradually concentrates on the edge of the defect. This stress concentration maybe the cause of the failure surgery which area size was larger than 10 mm [16], but this study did not simulate the heel-strike phase, the midstance and push-off phase of the ankle joints, and did not recorded the changes stress and displacement of the ankle when the talus osteochondral defect at these positions. Clinically, for the treatment of talus osteochondral defects, the defect diameter is less than 10mm as an indicator [17–19]. Clinical symptoms require surgical intervention. However, there is no relevant research on the stress and displacement of the ankle joint with an area defect area smaller than 10mm.

Therefore, our group used the three-dimensional finite element mechanics of different talus cartilage defects to simulate the changes in the stress and displacement of the ankle joint in the heel-strike phase, the midstance and push-off phase. We found that compared with normal talus cartilage, when the area defect is less than 6 mm*6 mm, the equivalent stress of the proximal talus, tibial cartilage and talus cartilage (Fig. 5) did not change significantly compared with the normal one, but when the area size was larger than 6 mm*6 mm, the stress increased with increasing area sizes of the defect in the midstance and push-off phases. The maximum stress can be increased more than 2–3 times, while had the little impact on the heel-strike phase. According to the motion mechanics of the ankle joint and the gait cycle, the heel-strike phase is the moment when the heel touches the ground, which is the beginning of the support

phase [20]. At this time, the front articular surface of the talus (area 1/2/3, Fig. 3) is contact with the tibia, and the defect area was in zone 4 (Fig. 3), which was located in the middle medial of the talus and the stress is small, so the changed of stress was not obvious in heel-strike phase; while in the midstance and push-off phases, the stress in the talus zone 4 increases and reaches the maximum value. The position of the talus is different during the movement of the ankle joint. We believe that this is the main reason why the biological stress had the different tendency.

The displacement of the talus (Fig. 6) indicates the overall stability of the ankle joint. Our study found that compared with the normal one, the changes of the talus movement of various areas of the talus osteochondral defect mainly occurred in the midstance and push-off phases, and the talus displacement in the heel-strike phase was small, and the change was not obvious; the talus displacement of were the same as the previous stress indexes in the midstance and push-off phases. When the defect area was less than 6 mm * 6 mm, we found that the difference between the displacement of the talus between the normal ankle joint was not obvious, when the defect area exceeded 6 mm * 6 mm, the talus displacement of the midstance and push-off phases gradually increased, and when the defect area was 12 mm * 12 mm, the talus displacements reached its maximum value, which were 8.4045 mm and 7.3983 mm respectively, which were significantly increased compared with the normal group, it was a positive growth trend. It was suggested that talus osteochondral defects have little effect on the stability of the ankle joint when the defect area is less than 6 mm * 6 mm. When the defect area is larger than 6 mm * 6 mm, it might cause ankle joint instability. We speculate that the reason for this result may be related to the anatomical structure of the talus it is wide in the front and it is narrow in the back. In the heel-strike phase, the ankle joint is in the dorsal position and the ankle joint is relatively stable; while in the midstance and push-off phases, the stability of the ankle joint is reduced, so the biomechanical impact of the talus osteochondral defect is more obvious.

Therefore, for OLT, its impact on joint stress and stability should be actively considered, so that targeted treatment can be made to reduce the damage caused by the defect area to the ankle joint. If the defect area is less than 6 mm* 6 mm, the stress and displacement of the ankle joint are not very obvious. Appropriate treatment should be taken according to the patient's clinical manifestations, and conservative treatment methods can be considered. For the defect area larger than 6 mm * 6 mm, because the stress and displacement of the ankle joint are showing a positive growth trend, which has a great impact on the stability of the joint, we can consider the surgical treatment. Our study was more accurate than the defect area of $\leq$ 10mm diameter mentioned in the previous literature. Minimize the stress changes of the ankle joint and restore the stability of the ankle joint as soon as possible, and reduce the damage to the ankle joint during later weight-bearing activities.

This study has limitation. Because finite element analysis just simplifies the ankle joint model, so it cannot fully replicate the characteristics of the human ankle joint. Further biomechanical tests and clinical trials are needed to verify In the next step of the study, we are ready to further verify the experimental results of this experiment in clinical samples or cadaver samples.

5. Conclusions

The effect of cartilage area size defects of the talus on the biomechanics of the ankle is obvious especially in the midstance phase and push-off phase. When the defect size reaches 6 mm * 6 mm, the most obvious change in the stability of the ankle joint occurs, and the effect does not increase linearly with the increase in the depth of the defect. For the defect area larger than 6 mm * 6 mm, because the stress and displacement of the ankle joint are showing a positive growth trend, which has a great impact on the stability of the joint, we can consider the surgical treatment.

List Of Abbreviations

finite element analysis (FEA); Osteochondral lesion of the talus (OLT);

Declarations

Ethical approval

This study was approved by the institutional review board of the Chinese PLA General Hospital.

Consent for publication

Written informed consent for publication was obtained from the participants.

Author contributions

Conceptualization, M.W and PB.Y.; methodology, J.L.; software, J.L.,Y.L; validation, YZ.W., Y.W. and D.K.; formal analysis, J.L and Y.W.; investigation, YZ.W.; resources, D.K.; data curation, Y.W., DY.W, S.C; Ywriting—original draft preparation, J.L and YZ.W.; writing—review and editing, J.L and M.W.; visualization, PB.Y.; supervision, M.W and PB.Y.; project administration, J.L and W.M.; funding acquisition, W.M. All authors have read and agreed to the published version of the manuscript.

Availability of data and material

Data and materials were accessible in the case system at our department.

Competing Interests

All authors declare that they have no conflicts of interest concerning this study.

Funding

There is no funding to this study.

Acknowledgements

I would like to thank all authors for help and support in the process of data analysis and article writing, and thank my family for their selfless support to my work.

References

1. Kelly M, Bennett D, Bruce-Brand R, O'Flynn S, Fleming P. One week with the experts: a short course improves musculoskeletal undergraduate medical education. J Bone Joint Surg Am. 2014 Mar 5;96(5):e39. doi: 10.2106/JBJS.M.00325. PMID: 24599211.
2. Hiller CE, Nightingale EJ, Raymond J, Kilbreath SL, Burns J, Black DA, Refshauge KM. Prevalence and impact of chronic musculoskeletal ankle disorders in the community. Arch Phys Med Rehabil. 2012 Oct;93(10):1801–7. doi: 10.1016/j.apmr.2012.04.023. Epub 2012 May 7. PMID: 22575395.
3. Choi WJ, Lee JW, Han SH, Kim BS, Lee SK. Chronic lateral ankle instability: the effect of intra-articular lesions on clinical outcome. Am J Sports Med. 2008 Nov;36(11):2167–72. doi: 10.1177/0363546508319050. Epub 2008 Jul 31. PMID: 18669983.
4. Giannini S, Vannini F. Operative treatment of osteochondral lesions of the talus dome: current concepts review. Foot Ankle Int. 2004;25:168–175.

5. Zengerink M,Struijs PA,Tol JL,et al. Treatment of osteo□ chondral lesions of the talus: a systematic review[J]. Knee Surg Sports Traumatol Arthrosc,2010,18(2): 238–246.
6. Murawski CD, Kennedy JG. Operative treatment of osteochondral lesions of the talus. J Bone Joint Surg Am. 2013 Jun 5;95(11):1045-54. doi: 10.2106/JBJS.L.00773. PMID: 23780543.
7. Ramponi L, Yasui Y, Murawski CD, Ferkel RD, DiGiovanni CW, Kerkhoffs GMMJ, Calder JDF, Takao M, Vannini F, Choi WJ, Lee JW, Stone J, Kennedy JG. Lesion Size Is a Predictor of Clinical Outcomes After Bone Marrow Stimulation for Osteochondral Lesions of the Talus: A Systematic Review. Am J Sports Med. 2017 Jun;45(7):1698–1705. doi: 10.1177/0363546516668292. Epub 2016 Nov 16. PMID: 27852595.
8. Rungprai C,Tennant JN,Gentry RD,et al. Management of osteochondral lesions of the talar dome[J]. Open Or□ thopJ,2017:743–761.
9. Li J, Wei Y, Wei M. Finite Element Analysis of the Effect of Talus Osteochondral Defects of Different Depths on Ankle Joint Stability. Med Sci Monit. 2020 Aug 21;26:e921823. doi: 10.12659/MSM.921823. PMID: 32820745; PMCID: PMC7456163.
10. Choi WJ, Park KK, Kim BS, Lee JW. Osteochondral lesion of the talus: is there a critical defect size for poor outcome? Am J Sports Med. 2009 Oct;37(10):1974–80. doi: 10.1177/0363546509335765. Epub 2009 Aug 4. PMID: 19654429.
11. Ramponi L, Yasui Y, Murawski CD, Ferkel RD, DiGiovanni CW, Kerkhoffs GMMJ, Calder JDF, Takao M, Vannini F, Choi WJ, Lee JW, Stone J, Kennedy JG. Lesion Size Is a Predictor of Clinical Outcomes After Bone Marrow Stimulation for Osteochondral Lesions of the Talus: A Systematic Review. Am J Sports Med. 2017 Jun;45(7):1698–1705. doi: 10.1177/0363546516668292. Epub 2016 Nov 16. PMID: 27852595.
12. Hannon CP, Bayer S, Murawski CD, Canata GL, Clanton TO, Haverkamp D, Lee JW, O'Malley MJ, Yinghui H, Stone JW; International Consensus Group on Cartilage Repair of the Ankle. Debridement, Curettage, and Bone Marrow Stimulation: Proceedings of the International Consensus Meeting on Cartilage Repair of the Ankle. Foot Ankle Int. 2018 Jul;39(1_suppl):16S-22S. doi: 10.1177/1071100718779392. Erratum in: Foot Ankle Int. 2020 Oct 30;:1071100720967713. PMID: 30215307.
13. van Diepen PR, Dahmen J, Altink JN, Stufkens SAS, Kerkhoffs GMMJ. Location Distribution of 2,087 Osteochondral Lesions of the Talus. Cartilage. 2020 Sep 10:1947603520954510. doi: 10.1177/1947603520954510. Epub ahead of print. PMID: 32909458.
14. Elias I, Zoga AC, Morrison WB, Besser MP, Schweitzer ME, Raikin SM. Osteochondral lesions of the talus: localization and morphologic data from 424 patients using a novel anatomical grid scheme. Foot Ankle Int. 2007;28:154–161.
15. Hunt KJ, Lee AT, Lindsey DP, Slikker W 3rd, Chou LB. Osteochondral lesions of the talus: effect of defect size and plantarflexion angle on ankle joint stresses. Am J Sports Med. 2012 Apr;40(4):895–901. doi: 10.1177/0363546511434404. Epub 2012 Feb 23. PMID: 22366518.
16. Guo QW, Hu YL, Jiao C, Yu CL, Ao YF. Arthroscopic treatment for osteochondral lesions of the talus: analysis of outcome predictors. Chin Med J (Engl). 2010;123:296–300.
17. McGahan PJ, Pinney SJ. Current concept review: osteochondral lesions of the talus. Foot Ankle Int. 2010;31:90–101
18. Tol JL, Struijs PA, Bossuyt PM, Verhagen RA, van Dijk CN. Treatment strategies in osteochondral defects of the talus dome: a systematic review. Foot Ankle Int. 2000;21:119–126.
19. Zengerink M, Struijs PA, Tol JL, van Dijk CN. Treatment of osteo- chondral lesions of the talus: a systematic review. Knee Surg Sports Traumatol Arthrosc. 2010;18:238–246

20. Zeni JA Jr, Richards JG, Higginson JS. Two simple methods for determining gait events during treadmill and overground walking using kinematic data. Gait Posture. 2008 May;27(4):710–4. doi: 10.1016/j.gaitpost.2007.07.007. Epub 2007 Aug 27. PMID: 17723303; PMCID: PMC2384115.

Figures

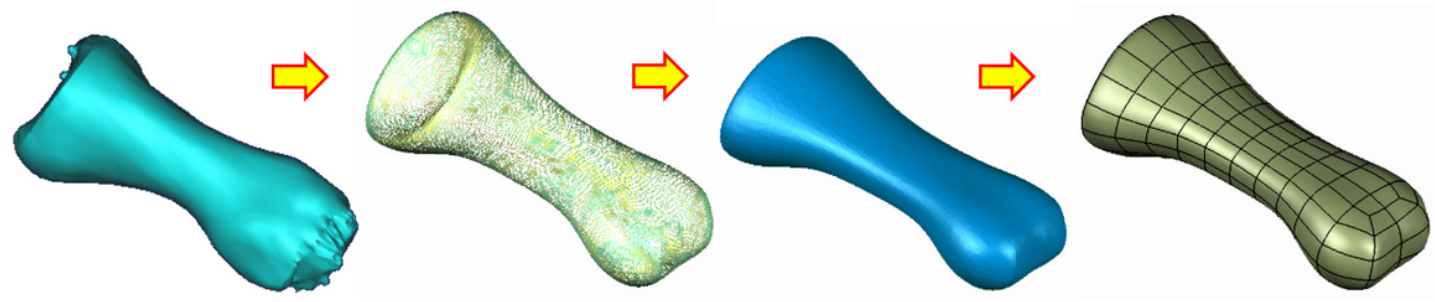

Figure 1 Diagram of processing the image with Geomagic

Figure 1

Diagram of image processing with Geomagic.

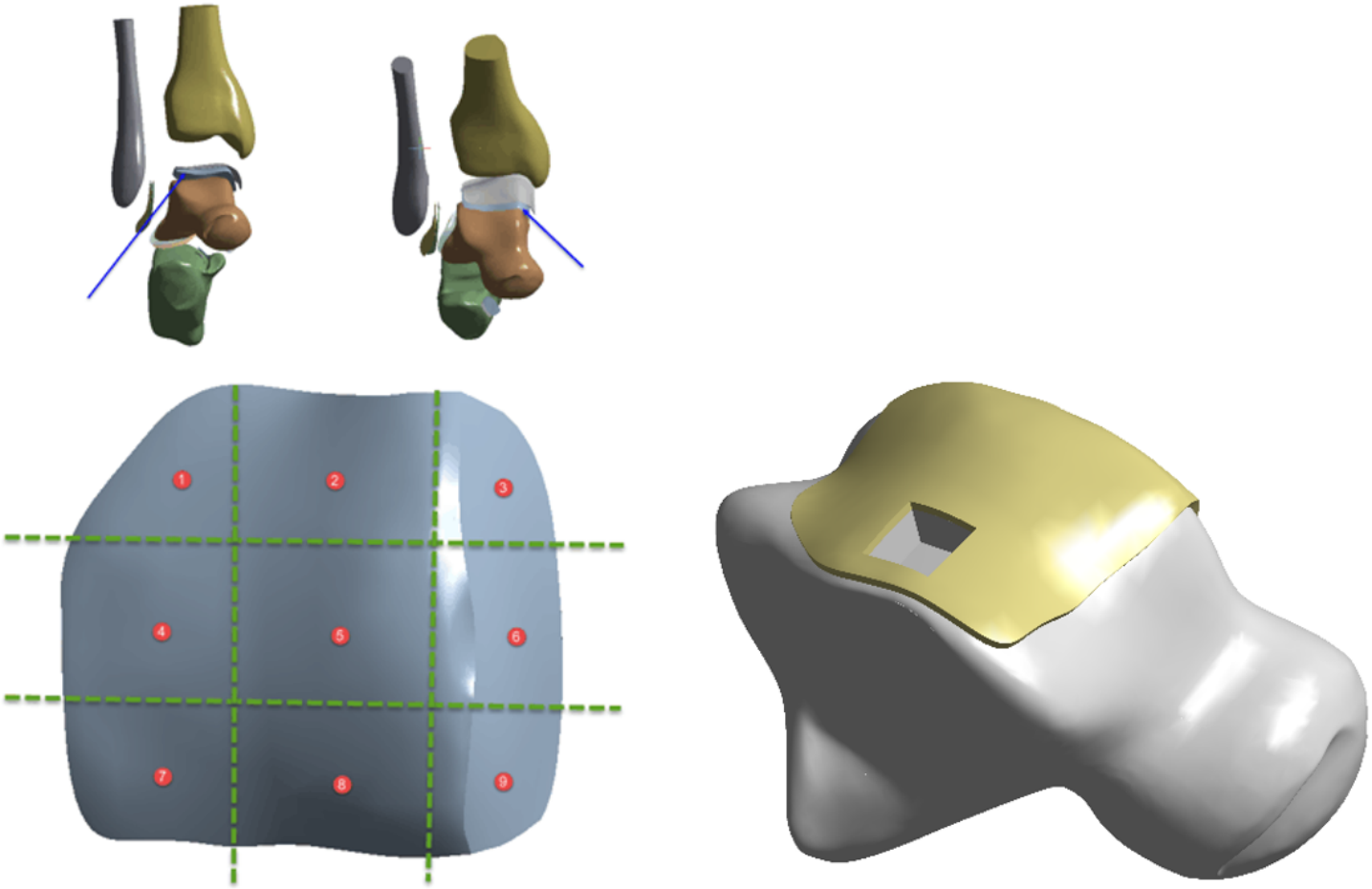

Figure 2

Location and depth of osteochondral loss.

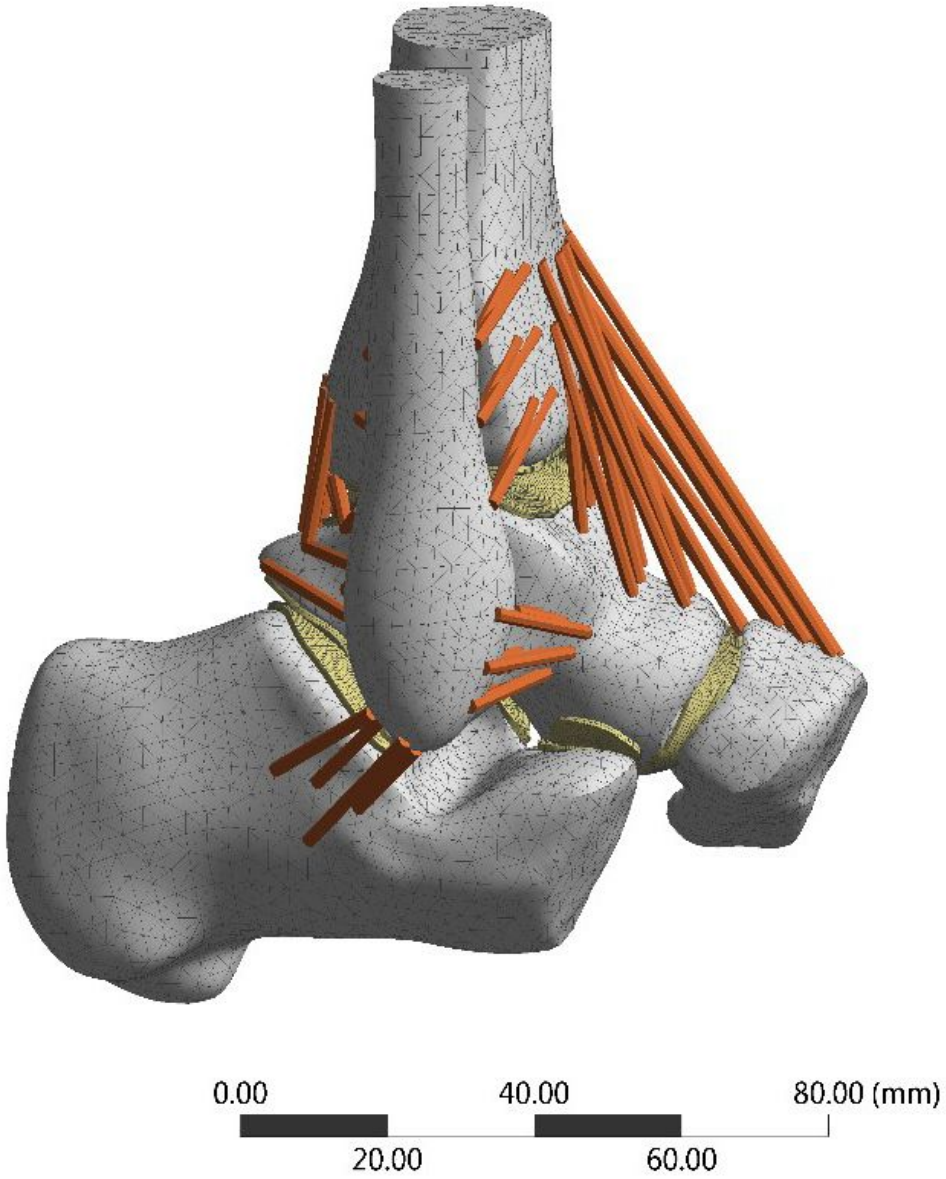

Figure 3

Mesh of ankle joint unit

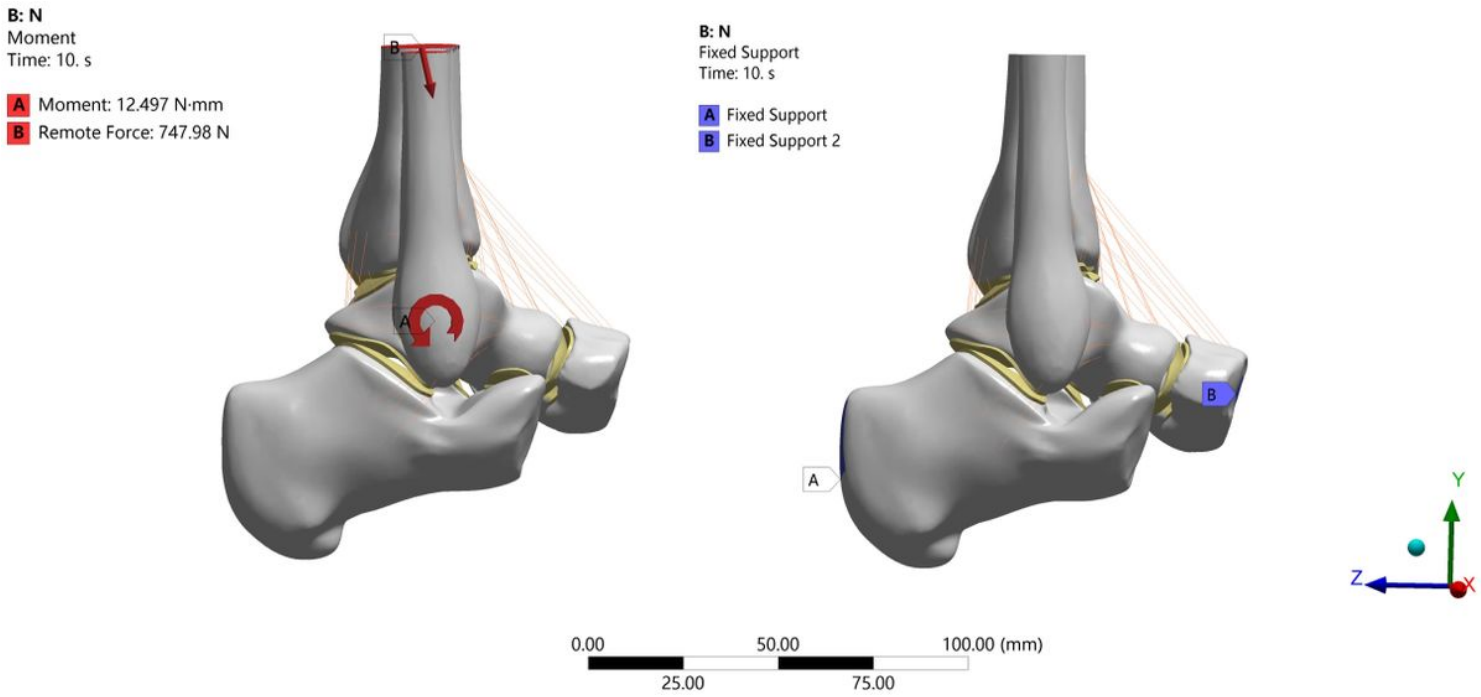

Figure 4

Mesh of ankle joint unit

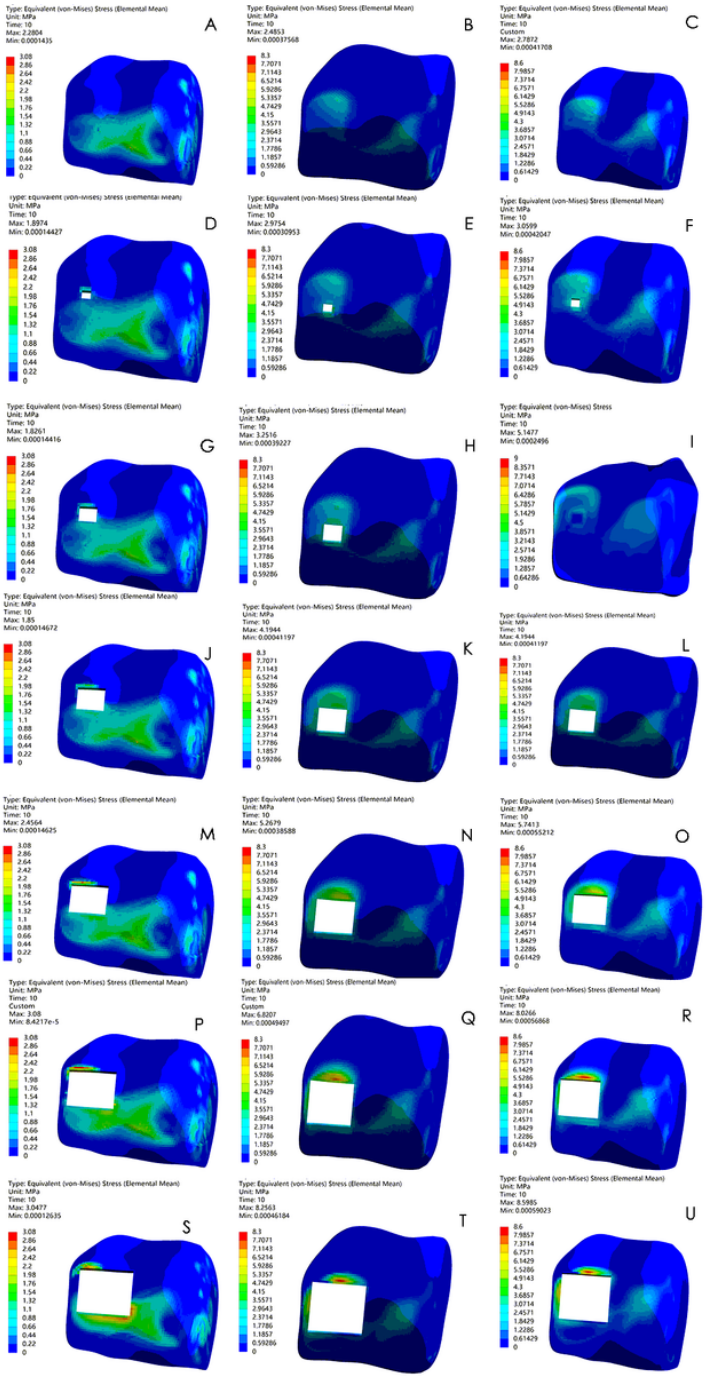

Figure 5

The equivalent stress of talus cartilage of 7 groups in heel-strike phase, the midstance and push-off phase: A-C Normal Group; D-F 2mm* 2mm Defect; G-I 4mm*4mm; J-L 6mm*6mm; M-O 8mm*8mm; P-R 10mm*10mm; S-U 12mm*12mm

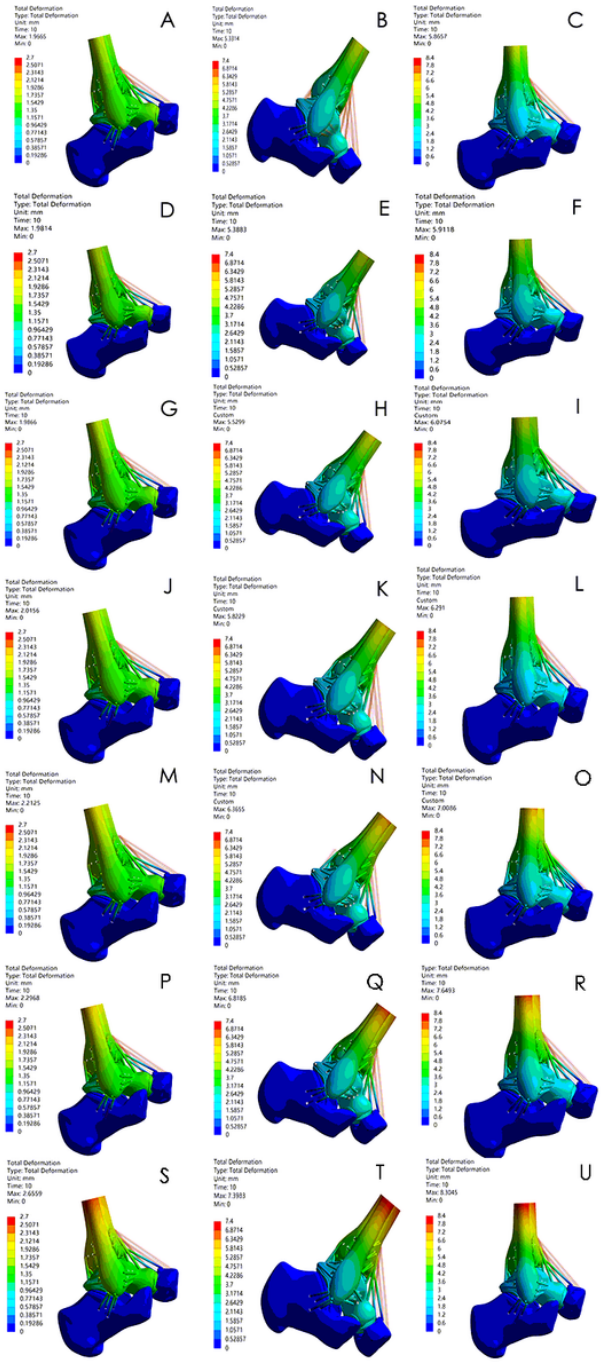

Figure 6

Displacement of the talus of 7 groups in heel-strike phase, the midstance and push-off phase: A-C Normal Group; D-F 2mm* 2mm Defect; G-I 4mm*4mm; J-L 6mm*6mm; M-O 8mm*8mm; P-R 10mm*10mm; S-U 12mm*12mm